ORIGINAL RESEARCH

Elevated Cellular Oxidative Stress in Circulating Immune Cells in Otherwise Healthy Young People Who Use Electronic Cigarettes in a Cross-Sectional Single-Center Study: Implications for Future Cardiovascular Risk

Theodoros Kelesidis, MD, PhD; Elizabeth Tran, BS; Sara Arastoo, MD; Karishma Lakhani, BS; Rachel Heymans [iD], MS; Jeffrey Gornbein, DrPH; Holly R. Middlekauff [iD], MD

BACKGROUND: Tobacco cigarettes (TCs) increase oxidative stress and inflammation, both instigators of atherosclerotic cardiac disease. It is unknown if electronic cigarettes (ECs) also increase immune cell oxidative stress. We hypothesized an ordered, "dose-response" relationship, with tobacco-product type as "dose" (lowest in nonsmokers, intermediate in EC vapers, and highest in TC smokers), and the "response" being cellular oxidative stress (COS) in immune cell subtypes, in otherwise, healthy young people.

METHODS AND RESULTS: Using flow cytometry and fluorescent probes, COS was determined in immune cell subtypes in 33 otherwise healthy young people: nonsmokers (n=12), EC vapers (n=12), and TC smokers (n=9). Study groups had similar baseline characteristics, including age, sex, race, and education level. A dose-response increase in proinflammatory monocytes and lymphocytes, and their COS content among the 3 study groups was found: lowest in nonsmokers, intermediate in EC vapers, and highest in TC smokers. These findings were most striking in $CD14_{dim}CD16^+$ and $CD14^{++}CD16^+$ proinflammatory monocytes and were reproduced with 2 independent fluorescent probes of COS.

CONCLUSIONS: These findings portend the development of premature cardiovascular disease in otherwise healthy young people who chronically vape ECs. On the other hand, that the COS is lower in EC vapers compared with TC smokers warrants additional investigation to determine if switching to ECs may form part of a harm-reduction strategy.

REGISTRATION: URL: https://www.clinicaltrials.gov; Unique identifier: NCT03823885.

Key Words: electronic cigarettes ■ monocytes ■ nicotine ■ reactive oxidative species ■ tobacco cigarettes

Oxidative stress and inflammation are implicated in the pathogenesis of most human diseases, including cardiovascular diseases.[1] Long-term exposure to excessive levels of reactive oxygen species (ROS) introduced through environmental exposures or through dysfunctional endogenous enzymatic systems overwhelm antioxidant defense systems, resulting in cellular damage and activation of circulating immune cells.[1,2] Activated immune cells, in turn, generate additional ROS, driving oxidation of lipoproteins and further

CLINICAL PERSPECTIVE

What Is New?

- Electronic cigarette (EC) vaping, which has grown to epidemic proportions among young people, is perceived as safer than tobacco cigarette smoking, but it remains unknown if otherwise healthy young EC vapers, like tobacco cigarette smokers, have increased oxidative stress and inflammation compared with nonsmokers.
- A dose-response increase in proinflammatory monocytes and lymphocytes, and their cellular oxidative stress content was found: lowest in nonsmokers, intermediate in EC vapers, and highest in tobacco cigarette smokers.

What Are the Clinical Implications?

- These findings portend the development of premature cardiovascular disease in otherwise healthy young people who chronically vape ECs.
- On the other hand, that the cellular oxidative stress is lower in EC vapers compared with tobacco cigarette smokers warrants additional investigation to determine if switching to ECs may form part of a harm-reduction strategy.

Nonstandard Abbreviations and Acronyms

COS	cellular oxidative stress
EC	electronic cigarette
NK	natural killer
TC	tobacco cigarette

recruitment of monocytes and macrophages, which then enter the vascular wall. Thus, ongoing oxidative stress and inflammation contribute to the initiation and progression of atherosclerotic vascular disease that may present decades later.

Tobacco cigarette (TC) smoking is the most prevalent modifiable risk factor for numerous human diseases, including atherosclerosis, in which oxidative stress and inflammation are known to play a critical role.[2,3] Over 90% of TC smokers begin smoking in their teens,[4] but TC-related diseases are insidious, presenting only after decades of TC smoking. Each puff of TC smoke contains 10^{15} free radicals[5] and >7000 different chemicals,[6] several of which are known toxicants or even carcinogens. Major prooxidant constituents in TC smoke generate cellular production of ROS when they interact with cellular enzymatic systems.[2] Innate and adaptive immune cells, such as myeloid cells (monocytes, macrophages, and dendritic cells), natural killer (NK) cells,

and lymphocytes (B and T cells) are activated by TC smoking,[7] and are also major sources of systemic oxidative stress.[8] Cigarette smoke activates leukocytes to release reactive oxygen and nitrogen species and contributes to development and progression of atherosclerotic cardiovascular disease through several mechanisms, such as secretion of proinflammatory cytokines and increased adherence of monocytes to the endothelium.[2,3] Although cellular oxidative stress (COS) has been studied in the setting of tobacco smoking and atherosclerosis, there is limited evidence regarding COS among electronic cigarette (EC) vapers.

ECs are the most rapidly rising tobacco product used in the United States today. EC aerosol, generated from heating, without combustion, solvents, flavors, and usually nicotine, contains significantly lower levels of toxicants compared with TC smoke.[9] Because of the long lag time for disease presentation, the health risks of ECs relative to TCs are unknown, yet ECs have been promoted as a smoking cessation, harm reduction, strategy. Alarmingly, largely because of the perceptions that ECs are safe, EC vaping has reached epidemic levels in never-smoking middle and high school students, with 30% of high school seniors (typically 17–18 years old) reporting EC vaping in the previous month.[10]

Although an urgent public health issue, the health risks associated with EC vaping, especially relative to TC smoking, remain unknown. The purpose of the current study was to pair sensitive flow cytometry with fluorescent probes to quantify the relative immune cell-type populations and their intracellular content of ROS in otherwise healthy young EC vapers compared with TC smokers, and nonsmokers. We hypothesized a continuum of oxidative stress and immune cell activation, essentially a "dose-response" relationship, with the "dose" defined as tobacco-product type (lowest in the nonsmokers, intermediate in the long-term EC vapers and highest in the long-term TC smokers), and the "response" defined as measures of immune cell subtypes and their COS.

METHODS

The data that support the findings of this study are available from the corresponding author on reasonable request. H.R.M. and T.K. had full access to all the data in the study and take responsibility for their integrity and the data analysis.

Materials

Flow cytometry reagents, including flow cytometry staining buffers and antibodies, were purchased from Biolegend. CellROX Green (catalog No. C10444) and

CellROX Deep Red (catalog No. C10442) were obtained from Thermo Scientific.

Study Population

Healthy male and female volunteers between the ages of 21 and 45 years were eligible for enrollment if they were long-term (≥1 year) (1) TC smokers, (2) EC vapers (no dual users), or (3) nonsmokers. Former TC smokers were eligible if >1 year had elapsed since quitting. End-tidal CO, elevated >10 ppm in smokers, was measured in EC vapers and nonsmokers to confirm none were surreptitiously smoking TCs. All participants were required to meet the following criteria: (1) nonobese (≤30 kg/m^2 body mass index); (2) no known health problems; (3) alcoholic intake ≤2 drinks per day and no regular illicit drug use, including marijuana, determined through screening questionnaire and urine toxicology testing; (4) no prescription medications (oral contraceptives allowed); and (5) not exposed to second-hand smoke, or using licensed nicotine replacement therapies. The experimental protocol was approved by the Institutional Review Board at the University of California, Los Angeles, and written, informed consent was obtained from each participant.

Experimental Protocol

After abstaining from caffeine, tobacco product use, and exercise for at least 12 hours, fasting participants reported to the UCLA Clinical Translational Research Center at the same time of day, ≈8 AM. Blood was drawn by trained medical assistants and prepared for flow cytometry and measurement of cotinine levels.

Flow Cytometry

Freshly isolated whole blood was immediately processed for flow cytometric determination of cellular ROS. COS was determined by the use of the CellROX Green Reagent, a measure of total (cytoplasmic and nuclear) cellular ROS,[11–13] and the use of the CellROX Deep Red Reagent, a measure of cytoplasmic cellular ROS.[14–16] The efficiency of CellROX Green to determine COS has previously been validated in several cells, including sperm, epithelial and melanoma cells, neurons, bacteria, and immune cells, such as macrophages.[17] The efficiency of CellROX Deep Red to assess COS has previously been validated in several cells, including sperm, endothelial and epithelial cells, hepatocytes, neurons, cardiomyocytes, and immune cells.[15] The CellROX Deep Red has been previously used to detect the ex vivo impact of cigarette smoke on cellular ROS by flow cytometry in spermatocytes.[16]

See Data S1 for detailed methods.

Determination of Plasma Cotinine Levels

The assay for plasma cotinine, using the method of chromatography/mass spectrometry, was run by the commercial laboratory, Quest Laboratories (Quest Diagnostics Incorporated, Madison, NJ), with a limit of quantitation of 2 ng/mL and a reference range in smokers of 16 to 145 ng/mL.

Statistical Analysis

We hypothesized an ordered, dose-response relationship of oxidative stress across the 3 study groups: lowest in nonsmokers, intermediate in long-term EC vapers, and highest in long-term TC smokers. We considered the "dose" to be the type of tobacco product used, and the "response" to be the immune cell subtype and its COS. To test this hypothesis, the *ordered trend* (F) *test* across the 3 ordered groups (nonsmokers, EC vapers, TC smokers) was computed under an ANOVA model.[18] Means±SEM are reported. If the overall trend P value or the overall ANOVA P value was ≤0.05, then the pairwise post hoc t test P values are reported between 2 groups (Fisher least significant difference criterion). The ordered trend test was considered statistically significant when $P \leq 0.05$. For continuous outcomes, examination of normal quantile plots and the Shapiro-Wilks statistic confirmed that the distributions followed the normal distribution. Overall and pairwise P values for comparing categorical covariates (sex, race, and education) across the 3 study groups were computed using the Fisher exact test.

Sample Size Calculation

Our primary outcomes are COS in proinflammatory monocytes, given their role in cardiovascular disease.[19] Given absence of data on monocyte frequencies or COS in immune cells in EC vapers, and based on data on frequencies of proinflammatory monocytes in otherwise healthy people without clinical disease,[20] a sample size of 9 participants per group (nonsmokers, EC vapers, and TC smokers) was sufficient to permit detection of a Δ of 2.9% with 80% power and 2-sided α=0.05. A total of 9 to 12 participants were included in each study group. This study, largely exploratory, is not powered to detect effect sizes with adjustments for multiple comparisons.[21,22] This is an interim report of our study registered at ClinicalTrials.gov (NCT03823885), which is a short-term exposure, crossover study.

RESULTS

Baseline Characteristics

A total of 33 participants, including 12 nonsmokers (age, 24.3±2.2 years; 5 women), 12 long-term EC vapers

Table. Baseline Characteristics

Characteristic	Nonsmokers (n=12)	EC Vapers (n=12)	TC Smokers (n=9)	P Value
Age, y	24.3±2.15	24.1±4.34	24.9±4.08	0.54
Sex (men/women)	7/5	8/4	4/5	0.61
Race				0.65
White	4	6	2	
Asian	4	5	3	
Black	2	0	1	
Hispanic	2	1	1	
Unknown	0	0	2	
BMI, kg/m^2	24±3.66	22.6±2.89	23.0±3.47	0.37
Plasma cotinine, ng/mL	0	85.0±126.2	58.0±39.5*	
Highest level education				1.0
<High school	0	0	0	
≥College	12	12	9	

Values are given as number or mean±SD. BMI indicates body mass index; EC, electronic cigarette; and TC, tobacco cigarette.
*P=0.34, EC vapers vs TC smokers.

(age, 24.1±4.3 years; 4 women), and 9 long-term TC smokers (age, 24.9±4.1 years; 5 women), participated in the study. Baseline characteristics of the 3 groups are shown in the Table. There were no differences among the groups in any variable, including age, sex, race, body mass index, or education level. All smokers and vapers used their tobacco product daily. Ten EC vapers reported using a "pod" device (eg, JUUL),
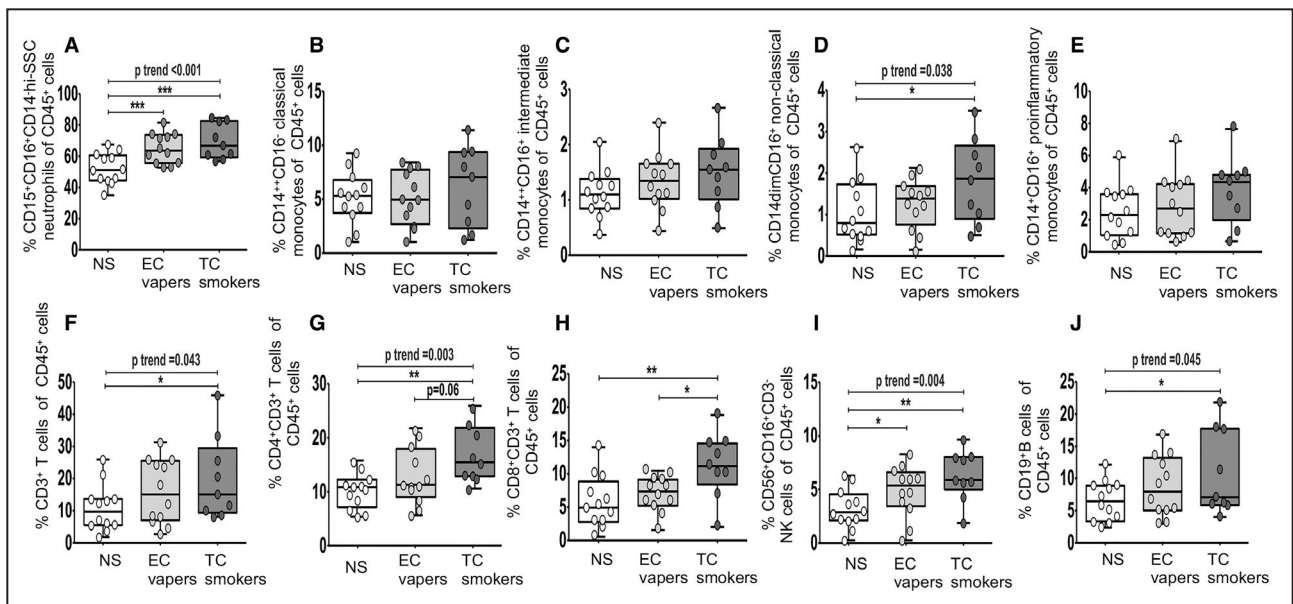
Figure 1. Frequency of immune cell types among smoker groups.
Flow cytometry was used to determine the percentage of different immune cell types in CD45$^+$ immune cells (**A** through **J**). The compared groups were nonsmokers (NSs; white), electronic cigarette vapers (EC vapers; light gray), and tobacco cigarette smokers (TC smokers; dark gray). Summary of data (% cellular marker$^+$ of parent population) is shown for CD45$^+$CD15$^+$CD16$^+$CD14$^-$hi-SSC neutrophils (**A**), CD45$^+$CD14^{++}CD16$^-$ classic monocytes (**B**), CD45$^+$CD14^{++}CD16$^+$ intermediate monocytes (**C**), CD45$^+$CD14dimCD16$^+$ nonclassic (patrolling or CD14$^+$CD16^{++}) monocytes (**D**), CD45$^+$CD14$^+$CD16$^+$ total proinflammatory monocytes (intermediate and nonclassic) (**E**), CD45$^+$CD3$^+$ T cells (**F**), CD45$^+$CD3$^+$CD4$^+$ T cells (**G**), CD45$^+$CD3$^+$CD8$^+$ T cells (**H**), CD45$^+$CD3$^-$CD56$^+$CD16$^+$ natural killer (NK) cells (**I**), and CD45$^+$CD19$^+$ B cells (**J**). Data represent box-and-whisker boxes that display the minimum, mean, and maximum (n=9–12 participants per group). The ANOVA statistical test was used to compare 3 groups, and the t test was used to compare 2 groups. The trend P analysis tested the continuum of the difference in measures among groups in an ordered direction (NSs→EC vapers→TC smokers). *P<0.05, **P<0.01, ***P<0.001.
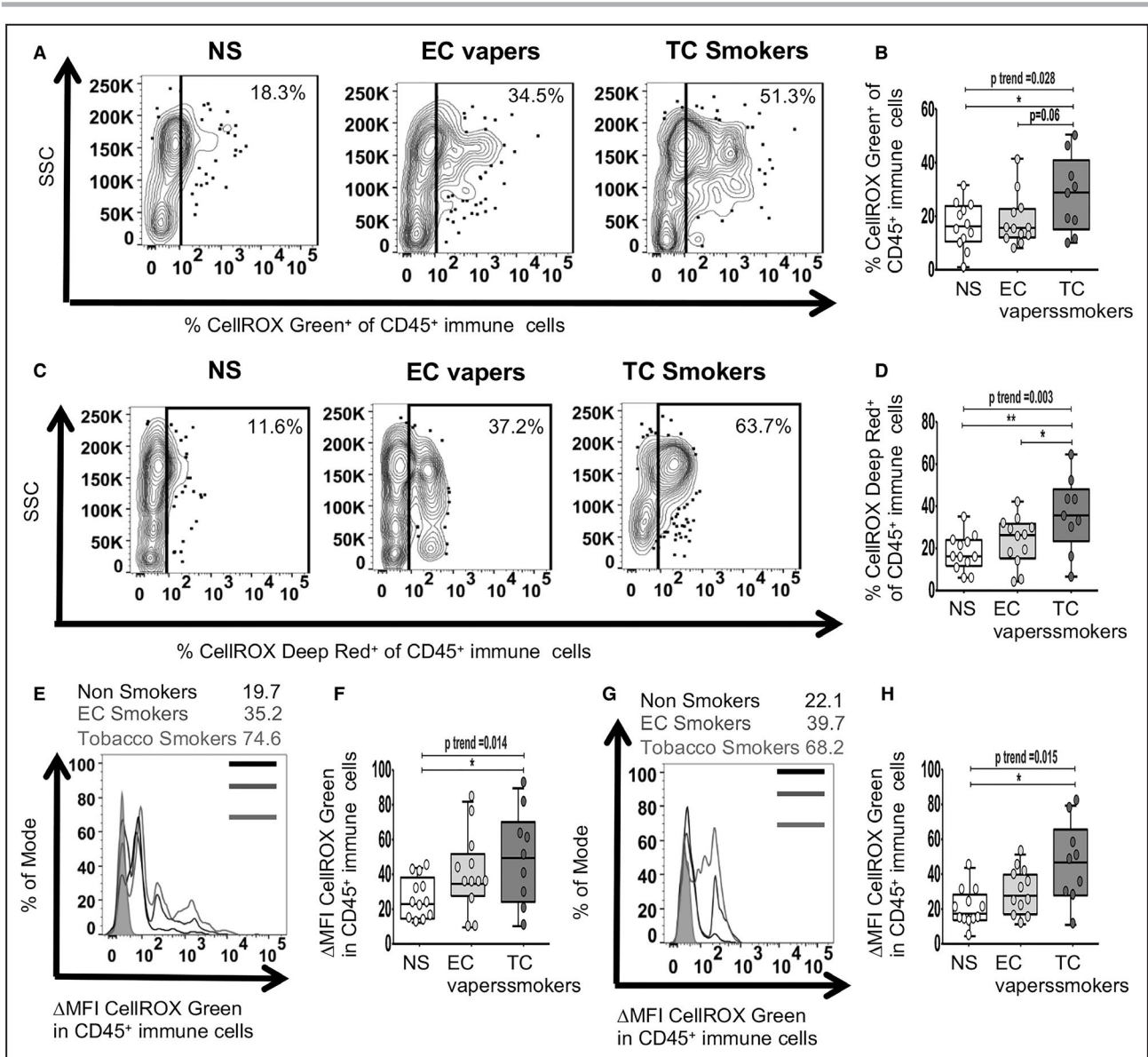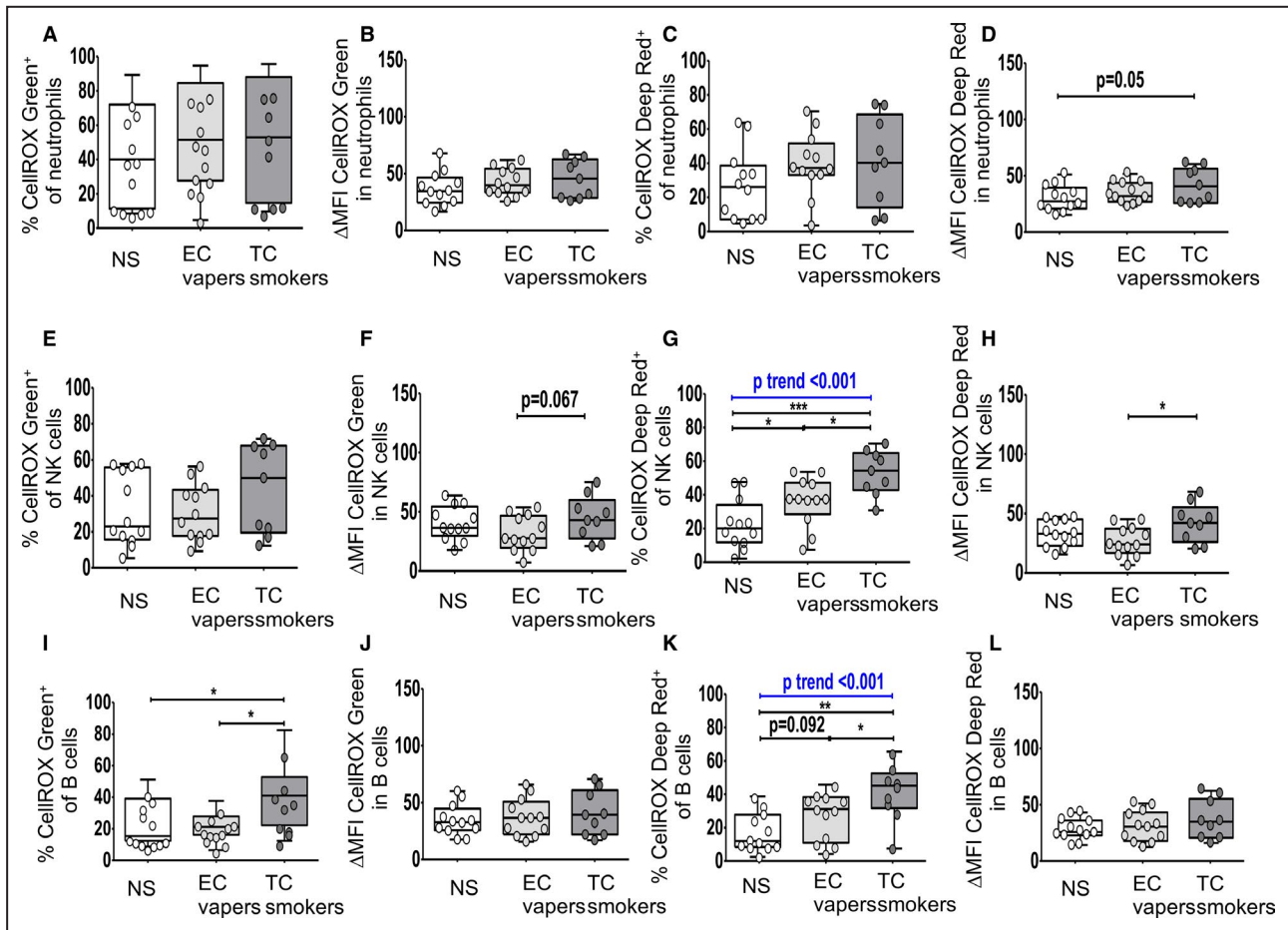
Figure 2. Cellular oxidative stress in CD45⁺ immune cells among smoker groups.
Flow cytometry was used to determine total (nuclear and cytoplasmic) and cytoplasmic reactive oxygen species. The compared groups were nonsmokers (NSs; white), electronic cigarette vapers (EC vapers; light gray), and tobacco cigarette smokers (TC smokers; dark gray). Representative data of percentage of immune (CD45⁺) cells that had positive staining for CELLROX Green among compared groups are shown (**A**). Summary of data for (**A**) is shown (**B**). Representative data of percentage of CD45⁺ cells that had positive staining for CELLROX Deep Red among compared groups are shown (**C**). Summary of data for **C** is shown (**D**). Representative data of CellROX Green change in mean fluorescence intensity (ΔMFI) in CD45⁺ cells are shown (**E**). Fluorescence intensity of a positive cell population was compared with a negative cell population (fluorescence minus one negative control for staining) (ΔMFI). Summary of data for **E** is shown (**F**). Representative data of CellROX Deep Red ΔMFI in CD45⁺ cells is shown (**G**). Summary of data for **G** is shown (**H**). Data represent box-and-whisker boxes that display the minimum, mean, and maximum (n=9–12 participants per group). The ANOVA statistical test was used to compare 3 groups, and the *t* test was used to compare 2 groups. The trend *P* analysis tested the continuum of the difference in measures among groups in an ordered direction (NSs→EC vapers→TC smokers). *$P<0.05$, **$P<0.01$. SSC indicates side scatter.

and one each used a "mod" or a "cigalike" device; all EC vapers used flavored, nicotine-containing liquid. Plasma cotinine levels were not significantly different in TC smokers and EC vapers (58 versus 85 ng/mL, respectively; *P*=0.34), consistent with similar, and relatively light, smoking burden.

Immune Cell Subtypes

To assess the impact of long-term smoking on immune cells, we first determined the frequency of immune cell subtypes among smoking groups (Figure). Gating strategies for viability dye and antibody staining

Figure 3. Cellular oxidative stress in neutrophils, natural killer (NK) cells, and B cells among smoker groups.
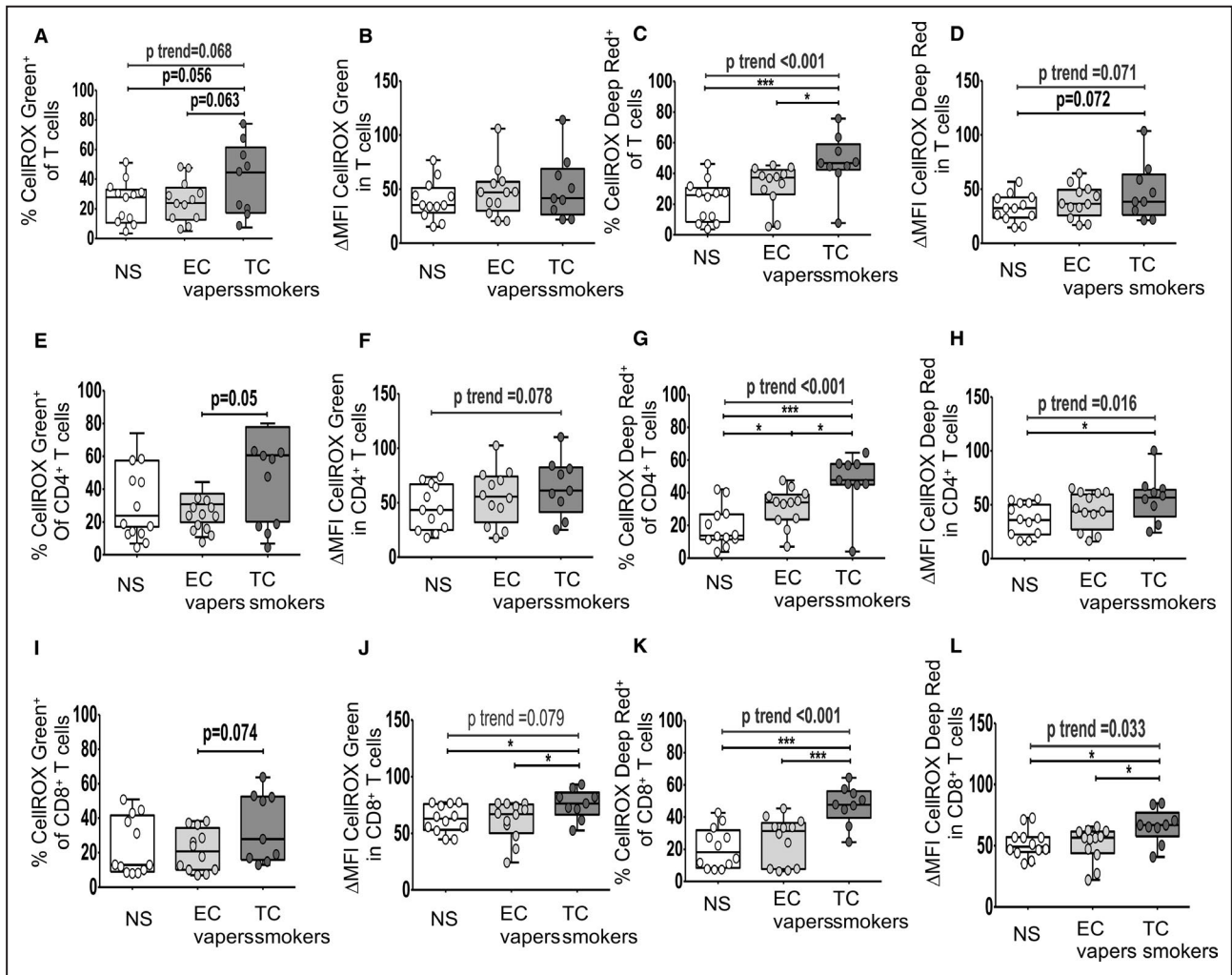
Flow cytometry was used to determine total (nuclear and cytoplasmic) and cytoplasmic reactive oxygen species. The compared groups were nonsmokers (NSs; white), electronic cigarette vapers (EC vapers; light gray), and tobacco cigarette smokers (TC smokers; dark gray). Summary data of percentage of immune cells that had positive staining for CELLROX Green (**A**, **E**, **I**) and CELLROX Deep Red (**C**, **G**, **K**) and for change in mean fluorescence intensity (ΔMFI) CellROX Green (**B**, **F**, **J**) and ΔMFI CellROX Deep Red in cells (**D**, **H**, **L**) among compared groups are shown for CD45+CD15+CD16+CD14−hi-SSC neutrophils (**A** through **D**), CD45+CD3−CD56+CD16+ NK cells (**E** through **H**), CD45+CD19+ B cells (**I** through **L**). Data represent box-and-whisker boxes that display the minimum, mean, and maximum (n=9–12 participants per group). The ANOVA statistical test was used to compare 3 groups, and the t test was used to compare 2 groups. The trend P analysis tested the continuum of the difference in measures among groups in an ordered direction (NSs→EC vapers→TC smokers). *P<0.05, **P<0.01, ***P<0.001.

are shown in Figure S1. Neutrophils, CD14dimCD16+ monocytes, and NK, T, and B cells were found in the lowest proportion in the nonsmokers, intermediate in the EC vapers, and in the greatest proportion in TC smokers and were lower in nonsmokers compared with TC smokers (Figure 1A through 1J).

COS in CD45+ Immune Cells

Given the lack of data on the impact of EC vaping on COS, we then determined the relative impact of long-term TC smoking or EC vaping on COS, as measured by flow cytometry using the fluorescent probes CellROX Green, a measure of total (cytoplasmic and nuclear) cellular ROS, and CellROX Deep Red, a

measure of cytoplasmic cellular ROS. There was a dose-response relationship among the 3 study groups for the percentage of CD45+ immune cells that were positive for total (Figure 2A and 2B) and cytoplasmic (Figure 2C and 2D) ROS (lowest in nonsmokers, intermediate in EC vapers, and greatest in TC smokers). In addition, the mean fluorescence intensity of total (Figure 2E and 2F) and cytoplasmic (Figure 2G and 2H) ROS in CD45+ immune cells also demonstrated this same, consistent dose-response relationship. Between-group comparisons consistently showed significantly greater COS in TC smokers compared with nonsmokers (Figure 2A through 2H). Cytoplasmic ROS was greater in TC smokers compared with EC vapers as well (Figure 2C and 2D).

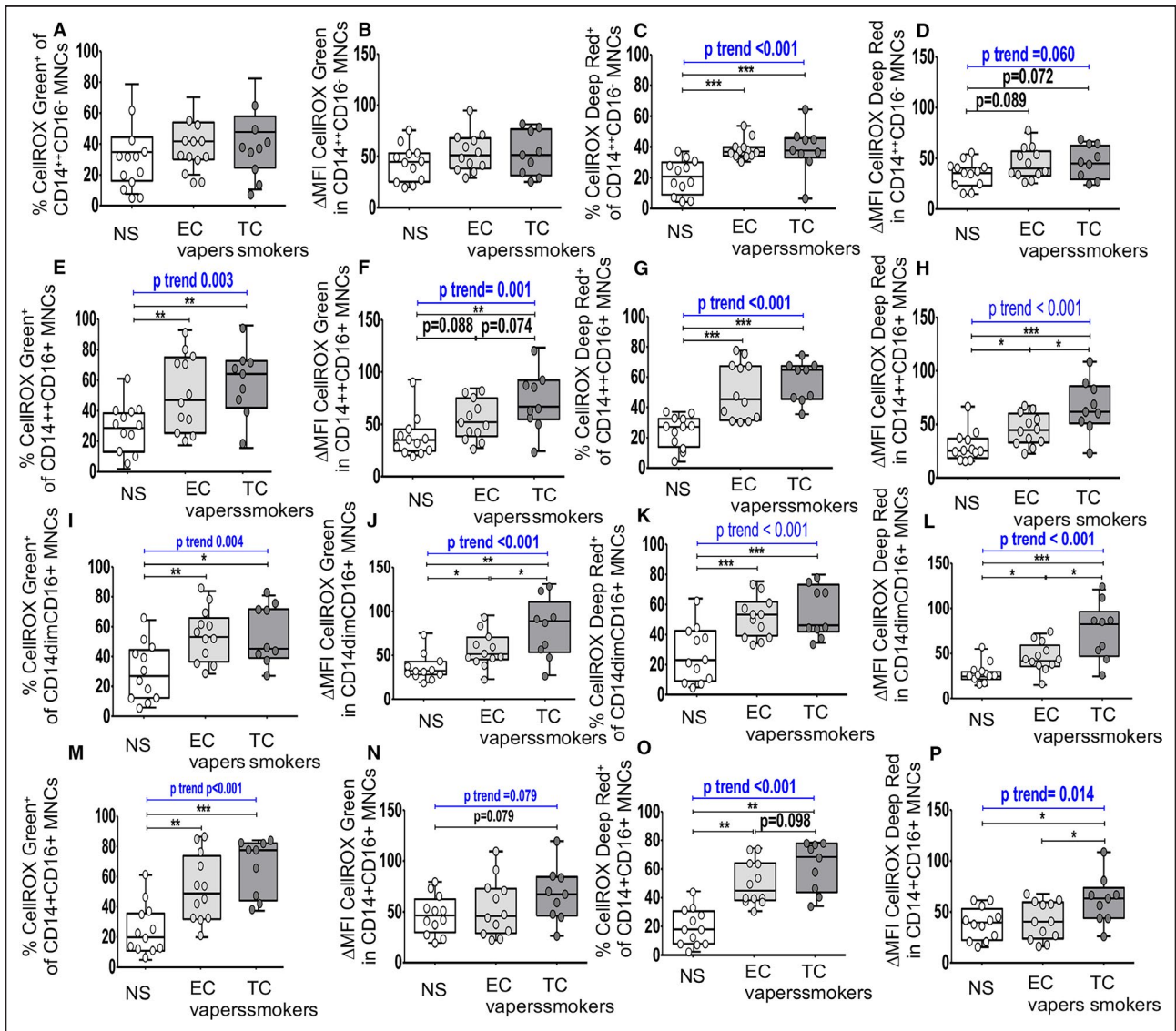**Figure 4. Cellular oxidative stress in T cell subsets among smoker groups.**
Flow cytometry was used to determine total (nuclear and cytoplasmic) and cytoplasmic reactive oxygen species. The compared groups were nonsmokers (NSs; white), electronic cigarette vapers (EC vapers; light gray), and tobacco cigarette smokers (TC smokers; dark gray). Summary data of percentage of immune cells that had positive staining for CELLROX Green (**A**, **E**, and **I**) and CELLROX Deep Red (**C**, **G**, and **K**) and for change in mean fluorescence intensity (ΔMFI) CellROX Green (**B**, **F**, and **J**) and ΔMFI CellROX Deep Red in cells (**D**, **H**, and **L**) among compared groups are shown for CD45+CD3+ T cells (**A** through **D**), CD45+CD3+CD4+ T cells (**E** through **H**), and CD45+CD3+CD8+ T cells (**I** through **L**). Data represent box-and-whisker boxes that display the minimum, mean, and maximum (n=9–12 participants per group). The ANOVA statistical test was used to compare 3 groups, and the t test was used to compare 2 groups. The trend P analysis tested the continuum of the difference in measures among groups in an ordered direction (NSs→EC vapers→TC smokers). *$P<0.05$, ***$P<0.001$.

COS in Specific Immune Cell Types

We then determined the impact of smoking exposures on COS among immune cell types (Figures 3 through 5). Group comparisons between TC smokers and EC vapers showed that there were no differences in ROS in neutrophils (Figure 3A through 3D). The proportion of B cells that had detectable total ROS (Figure 3I) and the proportion of NK (Figure 3G), B (Figure 3K), and total CD3+, CD4+, and CD8+ T cells (Figure 4C, 4G, and 4K) that had detectable cytoplasmic ROS were greater in TC smokers compared with EC vapers. Similar data were seen for the mean

content for cytoplasmic ROS in NK cells (Figure 3H) and for the mean content for total (Figures 4J and 5J) and cytoplasmic (Figures 4L and 5H, 5L, 5P) ROS in CD8+ T cells (Figure 4J and 4L) and proinflammatory monocytes (Figure 5H, 5J, 5L, and 5P). There were no differences in total ROS (Figure 3E and 3F) or the mean content for total (Figures 3J and 4B, 4F) and cytoplasmic (Figure 3L) ROS in NK (Figure 3E and 3F) and B cells (Figure 3L) in TC smokers compared with EC vapers.

Group comparisons between TC smokers and nonsmokers showed that the proportion of B cells (Figure 3I and 3K) and proinflammatory monocytes
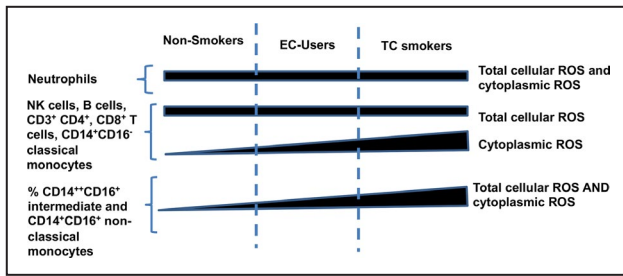
Figure 5. **Cellular oxidative stress in monocyte subsets among smoker groups.**
Flow cytometry was used to determine total (nuclear and cytoplasmic) and cytoplasmic reactive oxygen species. The compared groups were nonsmokers (NSs; white), electronic cigarette vapers (EC vapers; light gray), and tobacco cigarette smokers (TC smokers; dark gray). Summary data of percentage of immune cells that had positive staining for CELLROX Green (**A**, **E**, **I**, and **M**) and CELLROX Deep Red (**C**, **G**, **K**, and **O**) and for change in mean fluorescence intensity (ΔMFI) CellROX Green (**B**, **F**, **J**, and **N**) and ΔMFI CellROX Deep Red in cells (**D**, **H**, **L**, and **P**) among compared groups are shown for CD45$^+$CD15$^+$CD16$^+$CD14$^-$hi-SSC neutrophils (**A** through **D**), CD45$^+$CD3$^-$CD56$^+$CD16$^+$ natural killer cells (**E** through **H**), CD45$^+$CD19$^+$ B cells (**I** through **L**), and CD45$^+$CD3$^+$ T cells (**M** through **P**). Data represent box-and-whisker boxes that display the minimum, mean, and maximum (n=9–12 participants per group). The ANOVA statistical test was used to compare 3 groups, and the t test was used to compare 2 groups. The trend P analysis tested the continuum of the difference in measures among groups in an ordered direction (NSs→EC vapers→TC smokers). *$P<0.05$, **$P<0.01$, ***$P<0.001$. MNC indicates monocytes.

(Figure 5C, 5E, 5G, 5K, 5L, 5M and 5O) that had detectable cellular total (Figures 3I and 5E, 5L, 5M) and cytoplasmic (Figures 3K and 5C, 5G, 5K, 5O) ROS was greater in TC smokers compared with non-smokers. Similar results were seen for cytoplasmic ROS in NK (Figure 3G), B (Figure 3K), and T cells (Figure 4C), and T cell (Figure 4G and 4K) and monocyte (Figure 5C, 5G, 5K, and 5O) subsets. The mean cellular content for total (Figures 4J and 5F, 5J) and

cytoplasmic (Figures 4L and 5H, 5L, 5P) ROS was higher in CD8$^+$ T cells (Figure 4J and 4L) and proinflammatory monocytes (Figure 5F, 5H, 5J, 5L, and 5P) in TC smokers compared with nonsmokers. Similar trends (0.05<P<0.10) were observed in neutrophils (Figure 3D), NK cell (Figure 3F), T cell (Figure 4D), and monocyte subsets (Figure 5D and 5N) but were not consistent among independent readouts of COS. There were no other consistent differences in

Figure 6. Ordered, "dose-response" relationship in cellular oxidative stress among immune cell types and smoker groups, with tobacco-product type as "dose."
EC indicates electronic cigarette; NK, natural killer; ROS, reactive oxygen species; and TC, tobacco cigarette.

measures of COS in immune cell types between TC smokers and nonsmokers (Figures 3A through 3F, 3H, 3J, 3L, 4A, 4B, 4D, 4F, 4I, and 5A, 5B, 5D, 5N).

Group comparisons between EC vapers and nonsmokers showed that EC vapers had higher proportion of monocyte subsets (Figure 5C, 5G, 5K, and 5O) that had detectable total (Figure 5E, 5I, and 5M) and cytoplasmic (Figure 5C, 5G, 5K, and 5O) ROS compared with nonsmokers. Similar results were seen for cytoplasmic ROS in NK (Figure 3G) and CD4+ T cells (Figure 4G) and the mean cellular content for total (Figure 5J) and cytoplasmic (Figure 5H and 5L) ROS in proinflammatory monocytes. There were no differences in other measures of COS in other immune cell types between compared groups (Figures 3A through 3F, 3H through 3L, 4, and 5A, 5B, 5D, 5F).

There was a dose-response relationship among the 3 study groups for the mean percentage of NK (Figure 3G), B (Figure 3K), and T cells (Figure 4) and monocyte (Figure 5C, 5G, 5K, and 5O) subtypes with cytoplasmic ROS: lowest in the nonsmokers, intermediate in EC vapers, and greatest in TC smokers. The mean percentage of proinflammatory monocytes positive for total ROS (Figure 5E, 5I, and 5M) and the mean cellular content for total (Figure 5F, 5J, and 5N) and cytoplasmic ROS in proinflammatory monocytes (Figure 5H, 5L, and 5P) and T cell subtypes (Figure 4G and 4K) also followed this same pattern. The COS findings in different immune cell subpopulations and whether or not the dose-response relationship was observed are summarized in Figure 6.

DISCUSSION

To our knowledge, this is the first study to report alterations in the proportion of circulating innate and adaptive immune cells, as well as their COS content, in otherwise healthy young people who are long-term EC vapers or TC smokers compared with nonsmokers. Overall, we found a marked and consistent

dose-response increase in proinflammatory monocytes and lymphocytes, and their total cellular and cytoplasmic ROS content among the 3 study groups: lowest in the nonsmokers, intermediate in EC vapers, and highest in TC smokers. These findings were most striking in $CD14_{dim}CD16^+$ and intermediate in $CD14^{++}CD16^+$ proinflammatory monocytes and were reproduced with 2 independent fluorescent probes that determine total (CellROX Green) and cytoplasmic (CellROX Deep Red) cellular ROS.

Oxidative stress plays a major role in inflammation and cellular activation and is a major contributor to atherosclerotic cardiovascular disease.[1–3] The presence of excessive ROS has been termed the "convergent signaling hub" that underlies inflammatory diseases, including smoking-related atherosclerotic disease.[23] These findings of increased COS in key innate and adaptive immune cell subtypes portend the future development of premature atherosclerosis in otherwise healthy young people who chronically vape ECs.

TC smoking is a significant independent risk factor for many chronic and lethal diseases in humans.[1,2] Given the powerfully addictive nature of nicotine and the low rate of successful smoking cessation, ECs have been proposed as a potential harm-reduction strategy, with the ultimate goal of reducing morbidity and mortality while satisfying nicotine addiction.[24] ECs may emit fewer toxicants and carcinogens compared with TCs, but our findings confirm that their long-term use is associated with increased innate and adaptive immunity with increased COS. Although the proportion of immune cell subtypes, and their burden of COS, may be less in long-term EC vapers compared with TC smokers, it remains unproven and unknown if there is a "safe" level of chronic oxidative stress and inflammation.

Previous attempts to predict the adverse future health effects of ECs have been hampered by methodological limitations, such as relying on in vitro model systems or focusing on short-term, not long-term, EC exposure; in addition, most studies have been significantly underpowered.[25–29] In one of the few studies of health effects in long-term EC vapers, we reported an increased susceptibility to, but not actual presence of, chronic oxidative stress, estimated by low-density lipoprotein oxidizability, compared with healthy nonsmoking controls.[30] Traditional, clinical biomarkers of inflammation, including fibrinogen and CRP (C-reactive protein), were not elevated.[30] Admittedly, measurements of biomarkers in plasma lack sensitivity to elucidate the effects of ECs on oxidative stress and immune cell activation.

We found that COS was consistently elevated in $CD14_{dim}CD16^+$ and intermediate $CD14^{++}CD16^+$ proinflammatory monocytes of TC smokers and EC vapers compared with nonsmokers. $CD14^+CD16^+$ monocytes

are known contributors to atherosclerotic cardiovascular disease,[31–33] have increased chemotactic properties, and are potent secretors of interleukin-1, interleukin-6, and tumor necrosis factor-α.[34] However, their specific roles in atherosclerosis progression, lesion stability, and clinical events are uncertain. This monocyte subpopulation was also associated with increased vascular superoxide production in vascular dysfunction.[35] Consistent with our data, it has been shown that CD14+CD16+ monocytes have lower levels of antioxidant genes and increased aerobic respiration and ROS production capacities.[36] Given that oxidative stress is a known instigator of atherosclerosis,[2,3] it remains to be shown whether increased pro-oxidant capacity of CD14+CD16+ monocytes in the setting of EC vaping during lung chemotaxis may contribute to subsequent oxidative stress in arteries, portending the development of premature cardiovascular disease in otherwise healthy young people who chronically vape ECs.

The direct quantification of ROS is a valuable and promising biomarker that can reflect the disease process. However, given the short half-life of these species, their measurement in biological systems is complex. Determination of ROS has several methodological concerns, and global ROS measurements need to be avoided.[37] Identifying individual molecular targets of oxidation-reduction regulation is needed, and the complexity of COS can be studied only at the single cell level.[12] Approaches, such as mass spectrometry and spectrophotometric or luminescence methods, have major methodological limitations.[38] Although there is no single method that detects ROS that does not have limitations, the relative differences among different samples may be assessed reasonably and the bias of each method to detect ROS could be overcome by the evaluation of oxidative stress by using >1 criterion.[12] Flow cytometry is one of the most powerful tools for single-cell analysis of the immune system. Many fluorescent probes for the detection of reactive species have been developed in the last years, with a different degree of specificity and sensitivity.[12]

The CellROX Deep Red has been previously used to detect the ex vivo impact of TC smoke on cellular ROS by flow cytometry in spermatocytes.[16] The use of these fluorochromes for determination of COS in immune cells has previously been validated both in vitro[17] and in vivo.[39] The CellROX ROS detection reagents are bright and stable ROS sensors that offer significant advantages over existing ROS sensors because they are compatible with labeling in different media and can be used with fixatives.[40] This combined use has previously been described in nonimmune cells.[41] To the best of our knowledge, this study is pioneering in evaluating the efficiency of these probes in detecting ROS production among unique immune cell subsets.

Our study has limitations. Unlike animal studies, participants in human studies are heterogeneous. It is possible, but unlikely, that unmeasured, confounding differences exist among the 3 study groups, besides the obviously different smoking habits, to explain the marked and consistent differences in the proportion of immune cell subtypes and their oxidative stress. However, by any major demographic measure, including age, sex, race, and education level, the 3 study groups were markedly similar (Table). EC vaping is difficult to quantify objectively and then compare with commonly used measures of TC smoking (eg, number of cigarettes per day). Because all of our vapers used ECs with nicotine, plasma cotinine levels were used as an objective, quantifiable measure, common to both EC and TC users, that could be compared between groups to estimate relative tobacco product burden. Our study is a small single-center study, and not powered to detect effect sizes with adjustment for multiple comparisons. Rather, consistency, direction, and magnitude of the effect in conjunction with the nominal *P* values were considered to help distinguish true- and false-positive findings.[21,22] Accordingly, by leveraging the powerful technique of flow cytometry coupled to 2 different sensitive fluorescent probes, we were able to find a consistent dose-response relationship in COS among the 3 study groups that was repeated in both innate and adaptive immune cells. We acknowledge, however, that confirmation of these findings in additional participants is warranted.

In conclusion, our study is the first to report an increased proportion of proinflammatory monocytes/macrophages, NK cells, and T and B lymphocytes, in otherwise healthy young people who are long-term EC vapers compared with nonsmokers. This increased proportion of innate and adaptive immune cell subtypes is coupled with the finding that long-term EC vapers have elevated COS as well. Because low-grade oxidative stress and inflammation have been identified as the underlying mechanism that instigates and perpetuates atherosclerotic vascular disease that may manifest only decades later, these findings have important future health implications for young people who vape. On the other hand, that the COS is lower in long-term EC vapers compared with TC smokers is intriguing and warrants additional investigation to determine if switching to ECs may avoid activation of downstream detrimental cellular pathways, supporting their role as part of a harm-reduction strategy for cardiovascular disease. Future studies delineating the specific cellular pathways impacted in humans who chronically use ECs compared with TCs may provide further insights into their relative health risks, and whether switching to ECs will result in harm reduction.

ARTICLE INFORMATION

Affiliations

From the Division of Infectious Disease, Department of Medicine (T.K., R.H.), Division of Cardiology, Department of Medicine (E.T., S.A., K.L., H.R.M.), Department of Medicine (J.G.); and Department of Computational Medicine, David Geffen School of Medicine at UCLA, Los Angeles, CA (J.G.).

Sources of Funding

Disclosures

None.

Supplementary Materials

Data S1
Figure S1
References 42–70

REFERENCES

1. Sack MN, Fyhrquist FY, Saijonmaa OJ, Fuster V, Kovacic JC. Basic biology of oxidative stress and the cardiovascular system: part 1 of a 3-part series. *J Am Coll Cardiol*. 2017;70:196–211.

2. Csiszar A, Podlutsky A, Wolin MS, Losonczy G, Pacher P, Ungvari Z. Oxidative stress and accelerated vascular aging: implications for cigarette smoking. *Front Biosci (Landmark Ed)*. 2009;14:3128–3144.

3. Ambrose JA, Barua RS. The pathophysiology of cigarette smoking and cardiovascular disease: an update. *J Am Coll Cardiol*. 2004;43:1731–1737.

4. National Center for Chronic Disease Prevention and Health Promotion (US) Office on Smoking and Health. *The Health Consequences of Smoking—50 Years of Progress: A Report of the Surgeon General*. Atlanta, GA: Centers for Disease Control and Prevention (US); 2014.

5. Pryor WA, Stone K. Oxidants in cigarette smoke: radicals, hydrogen peroxide, peroxynitrate, and peroxynitrite. *Ann N Y Acad Sci*. 1993;686:12–27; discussion 27-28.

6. US Food & Drug Administration. Chemicals in Cigarettes: From Plant to Product to Puff. June 3, 2020. Available at: https://www.Fda.Gov/tobacco-products/products-ingredients-components/chemicals-cigarettes-plant-product-puff. Accessed June 23, 2020.

7. Qiu F, Liang CL, Liu H, Zeng YQ, Hou S, Huang S, Lai X, Dai Z. Impacts of cigarette smoking on immune responsiveness: up and down or upside down? *Oncotarget*. 2017;8:268–284.

8. Cathcart MK, Morel DW, Chisolm GM III. Monocytes and neutrophils oxidize low density lipoprotein making it cytotoxic. *J Leukoc Biol*. 1985;38:341–350.

9. Shahab L, Goniewicz ML, Blount BC, Brown J, McNeill A, Alwis KU, Feng J, Wang L, West R. Nicotine, carcinogen, and toxin exposure in long-term e-cigarette and nicotine replacement therapy users: a cross-sectional study. *Ann Intern Med*. 2017;166:390–400.

10. Miech R, Johnston L, O'Malley PM, Bachman JG, Patrick ME. Trends in adolescent vaping, 2017–2019. *N Engl J Med*. 2019;381:1490–1491.

11. Yang Z, Choi H. Single-cell, time-lapse reactive oxygen species detection in *E. Coli*. *Curr Protoc Cell Biol*. 2018;80:e60.

12. Kalyanaraman B, Darley-Usmar V, Davies KJ, Dennery PA, Forman HJ, Grisham MB, Mann GE, Moore K, Roberts LJ II, Ischiropoulos H. Measuring reactive oxygen and nitrogen species with fluorescent probes: challenges and limitations. *Free Radic Biol Med*. 2012;52:1–6.

13. McBee ME, Chionh YH, Sharaf ML, Ho P, Cai MW, Dedon PC. Production of superoxide in bacteria is stress- and cell state-dependent: a gating-optimized flow cytometry method that minimizes ROS measurement artifacts with fluorescent dyes. *Front Microbiol*. 2017;8:459.

14. Ray PD, Huang BW, Tsuji Y. Reactive oxygen species (ROS) homeostasis and redox regulation in cellular signaling. *Cell Signal*. 2012;24:981–990.

15. Pinke KH, Lima HG, Cunha FQ, Lara VS. Mast cells phagocyte *Candida albicans* and produce nitric oxide by mechanisms involving TLR2 and Dectin-1. *Immunobiology*. 2016;221:220–227.

16. Esakky P, Hansen DA, Drury AM, Cusumano A, Moley KH. Cigarette smoke-induced cell death of a spermatocyte cell line can be prevented by inactivating the aryl hydrocarbon receptor. *Cell Death Discov*. 2015;1:15050.

17. Wang H, Yang Y, Chen H, Dan J, Cheng J, Guo S, Sun X, Wang W, Ai Y, Li S, et al. The predominant pathway of apoptosis in THP-1 macrophage-derived foam cells induced by 5-aminolevulinic acid-mediated sonodynamic therapy is the mitochondria-caspase pathway despite the participation of endoplasmic reticulum stress. *Cell Physiol Biochem*. 2014;33:1789–1801.

18. Bartholomew DJ. A test of homogeneity for ordered alternatives. *Biometrika*. 1959;46:36–48.

19. Sager HB, Kessler T, Schunkert H. Monocytes and macrophages in cardiac injury and repair. *J Thorac Dis*. 2017;9:S30–S35.

20. Poitou C, Dalmas E, Renovato M, Benhamo V, Hajduch F, Abdennour M, Kahn JF, Veyrie N, Rizkalla S, Fridman WH, et al. CD14dimCD16+ and CD14+CD16+ monocytes in obesity and during weight loss: relationships with fat mass and subclinical atherosclerosis. *Arterioscler Thromb Vasc Biol*. 2011;31:2322–2330.

21. Feise RJ. Do multiple outcome measures require p-value adjustment? *BMC Med Res Methodol*. 2002;2:8.

22. Althouse AD. Adjust for multiple comparisons? It's not that simple. *Ann Thorac Surg*. 2016;101:1644–1645.

23. Chen Y, Zhou Z, Min W. Mitochondria, oxidative stress and innate immunity. *Front Physiol*. 2018;9:1487.

24. Chen J, Bullen C, Dirks K. A comparative health risk assessment of electronic cigarettes and conventional cigarettes. *Int J Environ Res Public Health*. 2017;14:382.

25. Carnevale R, Sciarretta S, Violi F, Nocella C, Loffredo L, Perri L, Peruzzi M, Marullo AG, De Falco E, Chimenti I, et al. Acute impact of tobacco vs electronic cigarette smoking on oxidative stress and vascular function. *Chest*. 2016;150:606–612.

26. Singh KP, Lawyer G, Muthumalage T, Maremanda KP, Khan NA, McDonough SR, Ye D, McIntosh S, Rahman I. Systemic biomarkers in electronic cigarette users: implications for noninvasive assessment of vaping-associated pulmonary injuries. *ERJ Open Res*. 2019;5:00182-2019.

27. Reidel B, Radicioni G, Clapp PW, Ford AA, Abdelwahab S, Rebuli ME, Haridass P, Alexis NE, Jaspers I, Kesimer M. E-cigarette use causes a unique innate immune response in the lung, involving increased neutrophilic activation and altered mucin secretion. *Am J Respir Crit Care Med*. 2018;197:492–501.

28. Scott A, Lugg ST, Aldridge K, Lewis KE, Bowden A, Mahida RY, Grudzinska FS, Dosanjh D, Parekh D, Foronjy R, et al. Pro-inflammatory effects of e-cigarette vapour condensate on human alveolar macrophages. *Thorax*. 2018;73:1161–1169.

29. Hiemstra PS, Bals R. Basic science of electronic cigarettes: assessment in cell culture and in vivo models. *Respir Res*. 2016;17:127.

30. Moheimani RS, Bhetraratana M, Yin F, Peters KM, Gornbein J, Araujo JA, Middlekauff HR. Increased cardiac sympathetic activity and oxidative stress in habitual electronic cigarette users: implications for cardiovascular risk. *JAMA Cardiol*. 2017;2:278–284.

31. Yoshida N, Yamamoto H, Shinke T, Otake H, Kuroda M, Terashita D, Takahashi H, Sakaguchi K, Hirota Y, Emoto T, et al. Impact of CD14(++) CD16(+) monocytes on plaque vulnerability in diabetic and non-diabetic patients with asymptomatic coronary artery disease: a cross-sectional study. *Cardiovasc Diabetol*. 2017;16:96.

32. Kapellos TS, Bonaguro L, Gemund I, Reusch N, Saglam A, Hinkley ER, Schultze JL. Human monocyte subsets and phenotypes in major chronic inflammatory diseases. *Front Immunol*. 2019;10:2035.

33. Rogacev KS, Cremers B, Zawada AM, Seiler S, Binder N, Ege P, Grosse-Dunker G, Heisel I, Hornof F, Jeken J, et al. CD14++CD16+ monocytes independently predict cardiovascular events: a cohort study of 951 patients referred for elective coronary angiography. *J Am Coll Cardiol*. 2012;60:1512–1520.

34. Cros J, Cagnard N, Woollard K, Patey N, Zhang SY, Senechal B, Puel A, Biswas SK, Moshous D, Picard C, et al. Human CD14dim monocytes patrol and sense nucleic acids and viruses via TLR7 and TLR8 receptors. *Immunity*. 2010;33:375–386.

35. Urbanski K, Ludew D, Filip G, Filip M, Sagan A, Szczepaniak P, Grudzien G, Sadowski J, Jasiewicz-Honkisz B, Sliwa T, et al. CD14(+)CD16(++) "nonclassical" monocytes are associated with endothelial dysfunction in patients with coronary artery disease. *Thromb Haemost*. 2017;117:971–980.

36. Zhao C, Tan YC, Wong WC, Sem X, Zhang H, Han H, Ong SM, Wong KL, Yeap WH, Sze SK, et al. The CD14(+/low)CD16(+) monocyte subset is more susceptible to spontaneous and oxidant-induced apoptosis than the CD14(+)CD16(-) subset. *Cell Death Dis*. 2010;1:e95.

37. Brandes RP, Rezende F, Schroder K. Redox regulation beyond ROS: why ROS should not be measured as often. *Circ Res*. 2018;123:326–328.

38. Dikalov SI, Harrison DG. Methods for detection of mitochondrial and cellular reactive oxygen species. *Antioxid Redox Signal*. 2014;20:372–382.

39. Tanase M, Urbanska AM, Zolla V, Clement CC, Huang L, Morozova K, Follo C, Goldberg M, Roda B, Reschiglian P, et al. Role of carbonyl modifications on aging-associated protein aggregation. *Sci Rep*. 2016;6:19311.

40. Bone B, Seredick B, Olszowy M. Reactive oxygen probes—a broad range of colors with easier labeling and compatibility with fixation: novel CellROX® reagents from Molecular Probes® (P3295). *J Immunol*. 2013;190:211.215.

41. Genov M, Kreiseder B, Nagl M, Drucker E, Wiederstein M, Muellauer B, Krebs J, Grohmann T, Pretsch D, Baumann K, et al. Tetrahydroanthraquinone derivative (+/-)-4-deoxyaustrocortilutein induces cell cycle arrest and apoptosis in melanoma cells via upregulation of p21 and p53 and downregulation of NF-kappaB. *J Cancer*. 2016;7:555–568.

42. Choi H, Yang Z, Weisshaar JC. Oxidative stress induced in *E. coli* by the human antimicrobial peptide ll-37. *PLoS Pathog*. 2017;13:e1006481.

43. de Castro LS, de Assis PM, Siqueira AF, Hamilton TR, Mendes CM, Losano JD, Nichi M, Visintin JA, Assumpcao ME. Sperm oxidative stress is detrimental to embryo development: a dose-dependent study model and a new and more sensitive oxidative status evaluation. *Oxid Med Cell Longev*. 2016;2016:8213071.

44. He Y, Li W, Zheng Z, Zhao L, Li W, Wang Y, Li H. Inhibition of protein arginine methyltransferase 6 reduces reactive oxygen species production and attenuates aminoglycoside- and cisplatin-induced hair cell death. *Theranostics*. 2020;10:133–150.

45. Schattauer SS, Bedini A, Summers F, Reilly-Treat A, Andrews MM, Land BB, Chavkin C. Reactive oxygen species (ROS) generation is stimulated by kappa opioid receptor activation through phosphorylated c-Jun N-terminal kinase and inhibited by p38 mitogen-activated protein kinase (MAPK) activation. *J Biol Chem*. 2019;294:16884–16896.

46. Rao VR, Lautz JD, Kaja S, Foecking EM, Lukacs E, Stubbs EB Jr. Mitochondrial-targeted antioxidants attenuate TGF-beta2 signaling in human trabecular meshwork cells. *Invest Ophthalmol Vis Sci*. 2019;60:3613–3624.

47. Skonieczna M, Hudy D, Poterala-Hejmo A, Hejmo T, Buldak RJ, Dziedzic A. Effects of resveratrol, berberine and their combinations on reactive oxygen species, survival and apoptosis in human squamous carcinoma (SCC-25) cells. *Anticancer Agents Med Chem*. 2019;19:1161–1171.

48. Chovancova B, Hudecova S, Lencesova L, Babula P, Rezuchova I, Penesova A, Grman M, Moravcik R, Zeman M, Krizanova O. Melatonin-induced changes in cytosolic calcium might be responsible for apoptosis induction in tumour cells. *Cell Physiol Biochem*. 2017;44:763–777.

49. Lilli NL, Revy D, Robelet S, Lejeune B. Effect of the micro-immunotherapy medicine 2LPARK((r)) on rat primary dopaminergic neurons after 6-OHDA injury: oxidative stress and survival evaluation in an in vitro model of Parkinson's disease. *Degener Neurol Neuromuscul Dis*. 2019;9:79–88.

50. Stelmashook EV, Genrikhs EE, Kapkaeva MR, Zelenova EA, Isaev NK. N-acetyl-L-cysteine in the presence of Cu(2+) induces oxidative stress and death of granule neurons in dissociated cultures of rat cerebellum. *Biochemistry (Mosc)*. 2017;82:1176–1182.

51. Isaev NK, Genrikhs EE, Aleksandrova OP, Zelenova EA, Stelmashook EV. Glucose deprivation stimulates Cu(2+) toxicity in cultured cerebellar granule neurons and Cu(2+)-dependent zinc release. *Toxicol Lett*. 2016;250-251:29–34.

52. Ahn HY, Fairfull-Smith KE, Morrow BJ, Lussini V, Kim B, Bondar MV, Bottle SE, Belfield KD. Two-photon fluorescence microscopy imaging of cellular oxidative stress using profluorescent nitroxides. *J Am Chem Soc*. 2012;134:4721–4730.

53. Rodrigues MB. An efficient technique to detect sperm reactive oxygen species: the CellROX Deep Red® fluorescent probe. *Biochem Physiol*. 2015;4:1–5.

54. Plaza Davila M, Martin Munoz P, Tapia JA, Ortega Ferrusola C, Balao da Silva CC, Pena FJ. Inhibition of mitochondrial complex I leads to decreased motility and membrane integrity related to increased hydrogen peroxide and reduced ATP production, while the inhibition of glycolysis has less impact on sperm motility. *PLoS One*. 2015;10:e0138777.

55. Korkmaz F, Malama E, Siuda M, Leiding C, Bollwein H. Effects of sodium pyruvate on viability, synthesis of reactive oxygen species, lipid peroxidation and DNA integrity of cryopreserved bovine sperm. *Anim Reprod Sci*. 2017;185:18–27.

56. Varela E, Rey J, Plaza E, Munoz de Propios P, Ortiz-Rodriguez JM, Alvarez M, Anel-Lopez L, Anel L, De Paz P, Gil MC, et al. How does the microbial load affect the quality of equine cool-stored semen? *Theriogenology*. 2018;114:212–220.

57. Saidani C, Hammoudi-Triki D, Laraba-Djebari F, Taub M. In vitro studies with renal proximal tubule cells show direct cytotoxicity of androctonus australis hector scorpion venom triggered by oxidative stress, caspase activation and apoptosis. *Toxicon*. 2016;120:29–37.

58. Celeghini ECC, Alves MBR, de Arruda RP, de Rezende GM, Florez-Rodriguez SA, de Sa Filho MF. Efficiency of CellROX deep red((R)) and CellROX orange((R)) fluorescent probes in identifying reactive oxygen species in sperm samples from high and low fertility bulls. *Anim Biotechnol*. 2019:1–7. https://doi.org/10.1080/10495398.2019.1654485.

59. Gallardo Bolanos JM, Balao da Silva CM, Martin Munoz P, Morillo Rodriguez A, Plaza Davila M, Rodriguez-Martinez H, Aparicio IM, Tapia JA, Ortega Ferrusola C, Pena FJ. Phosphorylated AKT preserves stallion sperm viability and motility by inhibiting caspases 3 and 7. *Reproduction*. 2014;148:221–235.

60. Wood JW, Bas E, Gupta C, Selman Y, Eshraghi A, Telischi FF, Van De Water TR. Otoprotective properties of mannitol against gentamicin induced hair cell loss. *Otol Neurotol*. 2014;35:e187–e194.

61. Annu AS, Kaur G, Sharma P, Singh S, Ikram S. Evaluation of the antioxidant, antibacterial and anticancer (lung cancer cell line A549) activity of *Punica granatum* mediated silver nanoparticles. *Toxicol Res (Camb)*. 2018;7:923–930.

62. Chong CM, Zheng W. Artemisinin protects human retinal pigment epithelial cells from hydrogen peroxide-induced oxidative damage through activation of ERK/CREB signaling. *Redox Biol*. 2016;9:50–56.

63. DeLoughery Z, Luczak MW, Zhitkovich A. Monitoring cr intermediates and reactive oxygen species with fluorescent probes during chromate reduction. *Chem Res Toxicol*. 2014;27:843–851.

64. Tormos AM, Talens-Visconti R, Bonora-Centelles A, Perez S, Sastre J. Oxidative stress triggers cytokinesis failure in hepatocytes upon isolation. *Free Radic Res*. 2015;49:927–934.

65. Murota Y, Tabu K, Taga T. Requirement of ABC transporter inhibition and Hoechst 33342 dye deprivation for the assessment of side population-defined C6 glioma stem cell metabolism using fluorescent probes. *BMC Cancer*. 2016;16:847.

66. Sung HK, Song E, Jahng JWS, Pantopoulos K, Sweeney G. Iron induces insulin resistance in cardiomyocytes via regulation of oxidative stress. *Sci Rep*. 2019;9:4668.

67. Leurgans TM, Bloksgaard M, Brewer JR, Bagatolli LA, Fredgart MH, Rosenstand K, Hansen ML, Rasmussen LM, Irmukhamedov A, De Mey JG. Endothelin-1 shifts the mediator of bradykinin-induced relaxation from NO to H2 O2 in resistance arteries from patients with cardiovascular disease. *Br J Pharmacol*. 2016;173:1653–1664.

68. Fang J, Zhao X, Li S, Xing X, Wang H, Lazarovici P, Zheng W. Protective mechanism of artemisinin on rat bone marrow-derived mesenchymal stem cells against apoptosis induced by hydrogen peroxide via activation of c-Raf-Erk1/2-p90(rsk)-CREB pathway. *Stem Cell Res Ther*. 2019;10:312.

69. Marrocco I, Altieri F, Peluso I. Measurement and clinical significance of biomarkers of oxidative stress in humans. *Oxid Med Cell Longev*. 2017;2017:6501046.

70. Rouaud F, Romero-Perez M, Wang H, Lobysheva I, Ramassamy B, Henry E, Tauc P, Giacchero D, Boucher JL, Deprez E, et al. Regulation of NADPH-dependent nitric oxide and reactive oxygen species signalling in endothelial and melanoma cells by a photoactive NADPH analogue. *Oncotarget*. 2014;5:10650–10664.

SUPPLEMENTAL MATERIAL

Data S1.

Supplemental Methods

Flow cytometry methods. Each CellROX dye was dissolved in DMSO at a final concentration of 5 mg/ml and stored at −80°C. Using the stock solution, dyes were diluted with PBS to achieve final staining concentrations. To minimize fluorescent quenching between whole blood proteins and fluorochromes, 100 µl of freshly isolated whole blood was centrifuged at 300 g for 5 min and the cell pellets were resuspended in PBS. To avoid artificial oxidation and to also study COS in neutrophils, we avoided red blood cell lysis and density gradient centrifugation that may artificially generate ROS. Cell pellets were stained with 5 µM CellROX Deep Red Reagent or 5 µM CellROX Green Reagent at 37C in the dark for 30 min.

After centrifugation at 300 g for 5 min, the cell pellets were resuspended in PBS and single cell suspensions were incubated with viability dye. LIVE/DEAD Fixable Aqua (a viability dye) for 405 nm excitation was used to exclude dead cells from analysis (Thermo Fisher Scientific). Aqua dye was dissolved in DMSO and stored at −80°C, according to the manufacturer's instructions. Just before use, Aqua dye was diluted 1:10 with PBS and used for staining. Aqua viability dye staining was performed by adding 2 µl of a diluted viability dye to 100 µl of cell suspension and then incubated at RT for 20 min in the dark. After washing twice with PBS, cells stained with Aqua dye were resuspended in 100 µl of PBS. The cell suspension was blocked at room temperature for 5 minutes for non-specific binding of antibodies with 5 µl of Fc blocker (Human TruStain FcX™, Biolegend) and for non-specific binding of fluorochromes with True-Stain Monocyte Blocker (Biolegend).

Appropriate antibodies were added to each tube and incubated in the dark for 20 minutes on ice. The following human antibodies were used: Brilliant Violet 570™ anti-human CD3 (clone UCHT1), Brilliant Violet 711™ anti-human CD4 (clone OKT4), PE/Cy7 anti-human CD8 (clone SK1), PE anti-human CD14 (clone HCD14), Brilliant Violet 650™ anti-human CD15 (SSEA-1) (clone W6D3), Brilliant Violet 605™ anti-human CD16 (clone 3G8), Brilliant Violet 510™ anti-

human CD19 (clone HIB19), Brilliant Violet 785™ anti-human CD45 (clone HI30) and PE/Dazzle™ 594 anti-human CD56 (NCAM) (clone 5.1H11). All antibodies were obtained from Biolegend. We chose antibodies labeled with fluorochromes that have as minimal excitation and emission overlap with CellROX® Green Reagent and CellROX® Deep Red Reagent as possible. The antibody staining of cells was performed after washes and separately than the staining of whole blood cell pellet with CellROX dyes to minimize interactions between fluorochromes that may confound interpretation of data. After 30 min, the cells were washed twice with PBS. After a short spin, the cells were suspended in 200 µL of ice-cold PBS buffer and transferred to fresh tubes for FACS analysis. Samples were acquired using an LSR Fortessa flow cytometer and FACSDiva software (BD Biosciences). Instrument settings (cytosettings) for each protocol were tailored with unique voltage and compensation matrices. Verify tubes were used to track instrument settings over time. Data were analyzed using FlowJo software. At least 30000 cells were acquired for each analysis, and each representative flow plot was repeated more than 3 times. Only live and singlet cells were chosen for analysis and gating (i.e., dead cells and aggregates were excluded).

To address the possible modulation effect of biochemical interactions (e.g. variable autofluorescence and uptake of a given concentration of fluorochromes) on detection of ROS formation among different participants, the MFI (Mean Fluorescence Intensity) related to fluorescence emission of the CellROX® Reagents was measured in single stain controls and also in fluorescence minus one (FMO) controls in the presence of a given concentration of the antibody staining cocktail. Two readouts of COS were used: i) % of cells that were positive for the CellROX fluorochromes (that determines the total cellular content of ROS); ii) the median cellular amount of ROS per cell type [median fluorescence intensity (MFI) of CellROX Green per cell type per sample minus the MFI of negative staining control]. Cellular ROS was determined in neutrophils, monocytes, lymphocytes and NK cells that carry ROS and contribute to systemic

OS and disease. The difference in fluorescence intensity compared to the negative control (DMFI or% positive cells for CellROX of parent cell population) was reported for each donor. Flow cytometry data among donors were obtained in parallel to avoid batch and autoxidative "aging" effects in stock solutions of dyes.

Gating strategies for viability dye and antibody staining are shown in Supplemental Figure 1. Total leukocytes were gated from all CD45 positive cells and gated cells included lymphocytes (low SSC) and monocytes (medium SSC), HLADR$^+$CD14$^+$ monocytes, CD19$^+$ B cells, CD3$^+$ T cells, CD4$^+$CD8$^-$ and CD4$^-$CD8$^+$ T cells and CD3$^-$CD19$^-$CD56$^+$ NK cells. Granulocytes gated by high side scatter (SSC^{high}) that were negative for the CD14 monocyte marker and were assessed for CD15 and CD16 to enumerate neutrophils (SSC^{high}, CD14$^-$, CD15$^+$CD16$^+$). Monocytes were separated into (1) CD14$^+$CD16$^-$ classical monocytes, (2) CD14$^+$CD16$^+$ intermediate monocytes, and (3) CD14^{lo}CD16$^+$ nonclassical monocytes. In cases where the antigens are expressed at low levels or do not have clearly defined positive populations, the position of the positive/negative gate was placed based on either different cell populations within the tube that were clearly negative, or the use of a fluorescence minus one (FMO) control tube.

Rationale to use CellROX Green and CellROX Deep Red for flow cytometric determination of cellular oxidative stress (COS)

CellROX Green. Cellular oxidative stress (COS) was determined by the use of the CellROX Green Reagent (absorption and emission maxima at 485/530 nm) which is non-fluorescent while in a reduced state and upon oxidation by reactive oxygen species (ROS) and subsequent binding to DNA, exhibits bright green fluorescence; it is a measure of total (cytoplasmic and nuclear) cellular ROS. CellROX Green (Thermo Scientific) is a proprietary, permeable, non-fluorescent, oxidation-sensitive dye that becomes fluorescent upon binding to DNA after being

oxidized by superoxide (O_1^-) and hydroxyl radical (•OH) and other species such as high-valence Fe centers in live cells[12, 42]. The CellROX green labels a series of intracellular compartments, including cytoplasm, nucleus, and mitochondria but is considered primarily a nuclear probe. DNA damage may be caused ROS-induced modifications of other molecules, such as lipids. Retention of activated dye in cells by binding to DNA, prevents loss of activated probe through leakage through damaged cell membranes[13]. Limited evidence suggests that CellROX Green may be a better detector for superoxide rather than hydrogen peroxide-induced hydroxyl radicals[13]. CellROX green may be more sensitive for detection of hydrogen peroxide-induced hydroxyl radicals compared to other probes like DCFH[43]. The efficiency of CellROX Green to determine COS has previously been validated in macrophages[17], sperm[43], epithelial cells[44-48], neurons[49-51], bacteria[11, 13, 42] and melanoma cells[41]. However, the CellROX Green is insensitive to oxidative nitrogen-containing radicals, hydrogen peroxide (H_2O_2) or to a variety of other oxidants including peroxynitrite ($ONOO^-$), NO, and hypochlorite (OCl^-).

CellROX Deep Red. Cytoplasmic cellular oxidative stress was determined by the use of the CellROX Deep Red Reagent (absorption and emission maxima at ~644/665 nm) which is non-fluorescent while in a reduced state and upon exhibits bright fluorescence upon oxidation by ROS in the cytoplasm; it is a measure of cytoplasmic cellular ROS. In contrast to CellROX green that binds to DNA when it oxidizes, CellROX deep red detects cytoplasmic free radicals that may underlie several complex mechanisms, including membrane lipid peroxidation, protein denaturation, and DNA damage, which may in turn induce apoptosis[14]. The CellROX Deep Red can detect ROS in fresh and fixed cells and seems to be more specific in detecting superoxide anion, nitroxides[52] and hydroxyl radical compared to other fluorescent probes[53]. The efficiency of CellROX Deep Red to assess COS has previously been validated in sperm cells[43, 54-59], epithelial cells[52, 60-63], hepatocytes[64], neurons[65], cardiomyocytes[66], melanoma

cells[41], endothelial[67], immune (such as mast cells[15]) and bone marrow-derived mesenchymal stem cells[68]. The CellROX deep Red has been previously used to detect the *ex vivo* impact of cigarette smoke on cellular ROS by flow cytometry in spermatocytes[16]. Limited evidence suggests that the hydrogen peroxide interferes with the CellROX Deep Red probe[57] which is catalase sensitive[67] and mainly identifies superoxide that may reflect intense mitochondrial activity[54-56, 66].

Rationale to use both CellROX Green and Deep Red. CellRox dyes are proprietary probes with unknown chemical structures but seem to be more specific and less sensitive in detecting ROS compared to other fluorochromes like dichlorofluorescein (DCF), dihydrorhodamine 113 (DHR113), dihydroethidium (DHE) and CellRox Orange[58, 63]. The use of these fluorochromes for determination of COS in immune cells has previously been validated both *in vitro*[17] and *in vivo*[39]. The CellROX Deep Red and Green probes can detect, simultaneously, the presence of superoxide anion and hydroxyl radical. The CellROX ROS detection reagents are bright and stable ROS sensors that offer significant advantages over existing ROS sensors because they are compatible with labeling in different media and can be used with fixatives[40]. It has been proposed that the bias of each method to detect ROS could be overcome by the evaluation of OS by using more than one criterion[66, 69, 70]. Thus, the combined use of both CellROX Deep Red and Green may better reflect total COS rather than use of either one alone. CellROX Green and Deep Red probes can differentiate between mitochondrial and cytosolic ROS. This combined use has previously been described in non-immune cells[41].

Figure S1. Gating strategy in flow cytometry experiments to determine the percent of different immune cells types that were positive for a combination of specific cellular markers.

Fluorescence intensity of a positive cell population was compared to a negative cell population (fluorescence minus one negative control for staining). Representative data of gates are shown: **1)** Single cells; →**2)** Cells (FSC/SSC) to exclude red blood cells and debris. Red blood cell lysis was not performed to avoid artificial oxidative stress during RBC lysis; →**3)** Viable cells were gated as negative stain for the SYTOX™ Blue dead cell stain; **4)** Immune cells were gated as CD45$^+$ on gate 3. From gate 4 the following gates were created: **5)** for CD19$^+$ B cells; **6)** for CD3$^+$ T cells; **7)** HLA-DR$^+$CD14$^+$ cells (monocytes; to exclude granulocytes, lymphocytes and NK cells); **8)** HLA-DR$^-$CD14$^-$ cells (to exclude monocytes). The following gates were also created: **9)** for CD56$^+$ NK cells (gated on CD3$^-$ cells on gate 6); **10)** for neutrophils (Hi SSC, CD15$^+$, CD14$^-$ HLA-DR$^-$; gated on 8); **11)** CD14^{++}CD16$^-$ classical monocytes; **12)** CD14^{++}CD16$^+$ intermediate monocytes; **13)** CD14$_{dim}$CD16$^+$ non-classical (patrolling or CD14$^+$CD16^{++}) monocytes; **14)** CD14$^+$CD16$^+$ total proinflammatory monocytes; **15)** CD3$^+$CD4$^+$ T cells (gated on 6); **16)** CD3$^+$CD8$^+$ T cells (gated on 6).

1) Single cells

FSC-H vs FSC-A

2) Cells

SSC-H vs SSC-A

3) Viable cells   Dead cells

SSC-H vs SYTOX-Blue (Viability dye)

5) CD19⁺ B cells

SSC-H vs CD19 BV510

4) CD45⁺ Immune cells

SSC-H vs CD45 BV785

6) CD3⁺ T cells

SSC-H vs CD3 BV 570

9)) CD3⁻CD56⁺ NK cells

SSC-H vs CD56 PE-Texas Red

10) Hi SSC, HLA-DR⁻ CD15⁺ cells

SSC-H vs CD15 BV650

7) HLA-DR⁺ CD14⁺ cells
8) HLA-DR⁻ CD14⁻ cells

CD14 PE vs HLA-DR APCCy7

11)CD14⁺⁺CD16⁻   12) CD14⁺⁺CD16⁺
13) CD14dim CD16⁺

CD14 PE vs CD16 BV605

15, 16) CD4⁺ and CD8⁺ T cells

CD4 BV711 vs CD8 PECy7